

LA-UR-97-**2592**

Title:

OXIDATION KINETICS OF PLUTONIUM IN AIR:  
CONSEQUENCES FOR ENVIRONMENTAL DISPERSAL

CONF-970907--

Author:

J.M. HASCHKE  
T.H. ALLEN  
J.C. MARTZ

RECEIVED

AUG 27 1997

OSTI

UNCLASSIFIED NOT UCNI

*Bj-Bj* JUL 08 1997  
FSS-16 date

Submitted to:

PROCEEDINGS OF ACTINIDE '97 MEETING IN  
JOURNAL OF ALLOYS AND COMPOUNDS

DISTRIBUTION OF THIS DOCUMENT IS UNLIMITED

**MASTER**

*pr*



**Los Alamos**  
NATIONAL LABORATORY

Los Alamos National Laboratory, an affirmative action/equal opportunity employer, is operated by the University of California for the U.S. Department of Energy under contract W-7405-ENG-36. By acceptance of this article, the publisher recognizes that the U.S. Government retains a nonexclusive, royalty-free license to publish or reproduce the published form of this contribution, or to allow others to do so, for U.S. Government purposes. The Los Alamos National Laboratory requests that the publisher identify this article as work performed under the auspices of the U.S. Department of Energy.

## **DISCLAIMER**

**Portions of this document may be illegible  
in electronic image products. Images are  
produced from the best available original  
document.**

# **Oxidation Kinetics of Plutonium in Air: Consequences for Environmental Dispersal**

John M. Haschke, Thomas H. Allen , Joseph C. Martz  
Los Alamos National Laboratory, P.O. Box 1663, Los Alamos , NM 87545, USA

## **Abstract**

Kinetic studies show that plutonium corrosion in air is catalyzed by plutonium hydride on the metal surface and suggest that the process has caused storage containers to fail. The catalyzed reaction initiates at 25°C, indiscriminately consumes both O<sub>2</sub> and N<sub>2</sub>, and transforms metal into a dispersible product at a 10<sup>7</sup>-10<sup>10</sup> faster rate ( $0.6 \pm 0.1 \text{ g Pu/cm}^2 \text{ min}$ ) than normal air oxidation. The catalyzed Pu+O<sub>2</sub> reaction advances into the metal at a linear rate of 2.9 m/h. Rate equations and particle size data, which are presented for catalyzed and atmospheric corrosion at temperatures up to 3500°C, provide a technical basis for more accurately assessing the dispersal hazard posed by plutonium metal.

## **Introduction**

Environmental dispersal of plutonium is a worldwide concern with possibilities of release from military and civilian sources. Most of the plutonium inventory exists as metal or oxide, two material forms with inherently different potentials for entrainment. Unlike oxide that often includes a large mass fraction of potentially dispersible particles, metal is not readily dispersed and presents a relatively low environmental hazard. However, the risk may be significantly enhanced by corrosion processes that transform the metal into plutonium-containing particles.

Corrosion rates of plutonium metal and alloys in dry and humid air are defined by early studies [1] and several recent investigations [2-6]. Kinetic behavior is strongly dependent on alloying and humidity below 400°C [6], but is independent of these factors at the  $500 \pm 25^\circ\text{C}$  ignition point of the metal [7]. The oxidation rate of ignited Pu is constant under static conditions that produce an oxygen-depleted boundary layer of N<sub>2</sub>,

but it has a 40 kJ/mol activation energy for the dynamic conditions of free fall [8]. The dynamic regime is entered during highly energetic events which form ignited metal droplets that explosively combust and release Pu vapor [9].

In this report, we present experimental results that account for cases in which rapid corrosion of plutonium in storage vessels lead to containment failure and release of plutonium [10-12]. In one case, corrosion of a 2.2 kg Pu casting contained in a screw-lid metal can, a sealed plastic contamination barrier, and an outer rim-seal can was complete within two years. Solid expansion during corrosion ruptured all containers. In a similar incident, 2.5 kg of cast Pu was welded in a steel cylinder, enclosed in plastic, and placed in a slip-lid can with a taped closure. After fourteen years in storage, external contamination was found during routine handling of the package and subsequent inspection revealed that the plastic barrier had failed and one end of the inner cylinder had ruptured. During disassembly of the package in a reduced oxygen (< 3 %) atmosphere, the cylinder became warm and its diameter increased by about 50% in 3 h.

A proposed explanation for these observations is hydride-catalyzed reaction of plutonium by air. Even when pumped by atmospheric pressure, insufficient oxygen reaches the metal through a small opening to cause rupture of an inner container, especially if the metal is surrounded by densely packed reaction product [12]. Kinetic data show that unrestricted oxidation of a typical casting by moist air at 25°C is expected to consume only 10-20 g of Pu over a two-year period in the presence of excess oxygen [6]. According to the proposed mechanism, radiolytic decomposition of the plastic degrades the barrier and produces hydrogen, which forms pyrophoric plutonium hydride. Exposure of the system to air upon failure of the plastic barrier results in rapid reaction.

The present study was initiated to investigate hydride enhancement of Pu corrosion by air and to evaluate the proposed mechanism. Experiments were designed to investigate the effects of several parameters on reactivity of metal-hydride systems, to define kinetic behavior, and to quantify properties relevant to environmental dispersal.

## **Experimental Methods**

A series of PVT (pressure-volume-temperature) experiments was conducted to define the chemistry and kinetics of the Pu-PuH<sub>2</sub> system upon exposure to air. The stainless steel PVT system consisted of heatable reaction, air/hydrogen source, and water source volumes that were interconnected by a vacuum-pressure manifold for handling and sampling of gases. For each test, a weighed specimen (25-50 g) of Pu-1 wt % Ga alloy was placed in the reaction vessel that was first evacuated and then backfilled with a desired amount of H<sub>2</sub>. After hydriding was complete, the air reservoir was filled with the required partial pressures of water and air, temperatures of the reactants were fixed, and the air was expanded into the evacuated vessel at 1.01 bar initial pressure. Reaction was monitored by measuring the time (t) dependence of pressure (P) and temperature (T). Reaction and air vessels were isolated and sampled for mass spectrometric (MS) analysis. Size distributions of solids were measured by sieving and light scattering methods.

The matrix of twenty-five experiments included three test configurations and several additional variables. In one configuration, 25 g samples of Pu were converted to hydride powder by slow addition of H<sub>2</sub> at a low temperature [13]. In configuration two, half of a 50 g Pu sample was hydrided using the same procedure. In configuration three, Pu was heated to 400°C and enough H<sub>2</sub> was added to form a 250-μm-thick layer of adherent hydride on the metal [13]. During tests with the first and second configurations, initial temperatures of the solid and the air were varied from 22 to 78°C and from 25 to 55°C, respectively. Partial pressures of H<sub>2</sub>O in the air varied from 0 to 30 mbar. In certain tests, 25 g of hydride was prepared by slow reaction of H<sub>2</sub> and a 25 g sample of Pu was added to the reactor under inert conditions before air exposure. Samples coated with adherent hydride were heated to 500°C and exposed to air or O<sub>2</sub> at 3.5 bar.

Results were derived from PVT and MS data. Reaction rates (R) are based on gas analyses, geometric metal area, and ideal reactions for formation of Pu<sub>2</sub>O<sub>3</sub> and PuN. Pu readily forms a solid-solution hydride, PuH<sub>x</sub> (2 < x < 3) [13]; PuH<sub>2</sub> is assumed to coexist

with the metal if  $x$  could not be defined. Reaction of nitrogen is defined by the  $N_2:O_2$  consumption ratio, which equals 3.71 if the two components of air react indiscriminately.

## Results and Discussion

Involvement of both  $O_2$  and  $N_2$  during  $PuH_x+air$  reaction is shown by tests in which only hydride was present or residual Pu metal did not react. The time dependencies of P and gas-phase T of a typical test are shown in Figure 1. The heat product causes thermal excursions of 100-125°C; the  $H_2$  product generates pressures in excess of the initial value over a period of 30 s. The negative pressure spike near 0.1 min results primarily from equipment design. Analysis of residual gases in the reactor (0.040 liter) and air reservoir (2.78 liters) shows 50-75 mole %  $H_2$  plus  $N_2$  and 2-7 mol %  $H_2$  plus air, respectively. Material-balance calculations show that the mole fractions of  $PuH_x$ ,  $PuN$ , and  $Pu_2O_3$  are 0.80-0.95, 0.03-0.15, and 0.02-0.05, respectively. Average  $x$  values of residual  $PuH_x$  approach 2.7. An average  $N_2:O_2$  ratio of  $1.6 \pm 0.5$  suggests that the  $PuH_x+air$  is somewhat unpredictable, but demonstrates that nitrogen is the primary reactant. Behavior was not altered by changes in initial temperature or humidity.

Though spontaneous reaction of  $PuH_x$  with  $O_2$  is expected, involvement of  $N_2$  is somewhat surprising. Early studies show that  $PuN$  is formed by the  $PuH_x+N_2$  reaction above 230°C [14]. Hydride temperatures probably exceed this value as a result of the  $PuH_x+O_2$  reaction. Each  $N_2$  reacts with  $PuH_2$  to form two  $H_2$ , but the observed amounts of  $H_2$  are much less than expected because product hydrogen is accommodated by increasing  $x$  of the hydride remaining within a reacting particle. The composition progressively increases as reaction occurs at the particle surface and continues until  $x$  approaches three[13]. Particle fracture and  $H_2$  release occur first for small particles with large surface area to volume ratios and cause the sluggish pressurization seen in Figure 1. Termination of reaction is promoted by the rising  $H_2$  pressure, a process that dilutes reactants and prevents entry of additional air.

Further reaction of air is possible if Pu metal and hydride coexist. Figure 2 shows P-t and T-t curves for reaction of a  $\text{Pu}+\text{PuH}_x$  mixture with air. For the first 30 s, the behavior closely parallels that for the  $\text{PuH}_x+\text{air}$  reaction, except that P never reaches 1 bar. Corrosion of Pu is evidenced by decreasing P and increasing T after 1 min. Analysis of residual gases shows air in the reservoir, an equimolar mixture of  $\text{H}_2$  and  $\text{N}_2$  in the reactor, and more than 95% of the initial hydrogen as  $\text{PuH}_x$ . The average  $\text{N}_2:\text{O}_2$  consumption ratio ( $3.4 \pm 0.1$ ) indicates indiscriminate reaction of metal to form  $\text{PuN}$  and  $\text{Pu}_2\text{O}_3$  in a ratio of 5.2:1. R decreases with P from  $0.75 \pm 0.09 \text{ g Pu/cm}^2 \text{ min}$  to an average of  $0.59 \pm 0.08 \text{ g Pu/cm}^2 \text{ min}$ . Initial T and humidity do not alter the behavior.

Results suggest that enhanced corrosion of Pu by  $\text{O}_2$  and  $\text{N}_2$  is catalyzed by adherent hydride on the surface of residual metal. Hydrogen formed by rapid reaction of the  $\text{PuH}_x$  layer with air advances into the metal at a rate accelerated by rapid transport of H in  $\text{PuH}_x$  [13]. Hydrogen from  $\text{PuH}_x$  particles slows the catalytic process and apparently stopped the reaction in several tests by filling the gas volume around the metal. In those tests, and in other configurations that restrict movement of  $\text{H}_2$  from the reaction zone, part of the  $\text{H}_2$  product must react before catalyzed corrosion can occur. Nucleation of the  $\text{Pu}+\text{H}_2$  reaction is temperature dependent, and though important, heat flow is an undefined factor. The uniqueness of adhering hydride is shown by the absence of catalytic corrosion in all tests in which separate pieces of metal were combined with hydride.

Effects of  $\text{PuH}_x$  particles and temperature are demonstrated by results of tests with hydride-coated metal. Observed P-t and T-t behavior parallels that for t greater than 1 min in Figure 2. Analytical data yield a  $\text{N}_2:\text{O}_2$  ratio of 3.7:1 and show that  $\text{H}_2$  did not form during the reaction or while products were heated at 500°C for 15 h. Initial and average R values are  $1.6 \pm 0.4$  and  $0.6 \pm 0.1 \text{ g Pu/cm}^2 \text{ min}$ , respectively. As defined by the slope of  $\ln R - \ln P$ , the exponents relating rate to air pressure at  $475 \pm 25^\circ\text{C}$  are 2.0 and 3.0 for P greater and less than 2.0 bar, respectively, suggesting that the reaction

mechanism is complex. Except for a change in solid volume, reacted specimens remained largely intact and consisted of a silver-gray product shell around a hydride core.

Reaction of the hydride-coated Pu with O<sub>2</sub> is violent. The metal reacted completely in less than 1 s and generated gas temperatures in excess of 1000°C. H<sub>2</sub> was not observed during reaction or during a several-hour period in O<sub>2</sub> at 500°C. Appearance of H<sub>2</sub>O after cooling to room temperature is consistent with catalytic properties of oxide [6]. The solid resembled that obtained in air with the hydride core anticipated for catalyzed reaction. P and T data taken after 1 s give an R of 78.1 g Pu/cm<sup>2</sup> min, or a linear rate of 2.93 m/h.

An estimate of the corrosion rate for unalloyed Pu (0.3 g Pu/cm<sup>2</sup> min) is based on observation of the storage vessel described in the introduction. This R is derived using approximate metal area, change in vessel volume during a 3 h period, and measured product density ( $6.5 \pm 0.5$  g/cm<sup>3</sup>). Agreement between this R and the average of 0.6 g Pu/cm<sup>2</sup> min for hydride-catalyzed corrosion suggests that the reaction is independent of alloying and that rapid failures of Pu storage containers were driven by that process.

Comparison of hydride-catalyzed reaction with normal air oxidation assists in defining hazards posed by Pu corrosion. Important considerations are the rate of corrosion and the particle size distribution of the product. The kinetics of uncatalyzed oxidation in air are described by Arrhenius relationships presented in Figure 3 and Table 1. Effects of alloying and moisture are seen below 400°C, a point at which all rates converge. Curves *a-d* for unalloyed Pu define the envelope of humidity effects between -25 to 200°C. Moisture dependencies of curve *c* for the transition region and of R within the envelope are given in a prior report [6]. Curves *e* and *f* indicate effects of moist and dry air on the Ga alloy, respectively. The somewhat uncertain transition to the ignition point at 500°C is described by Curve *g*. Self-sustained reaction of ignited metal at a T-independent rate under static conditions is shown by Curve *h*, and the authothermic reaction of an ignited Pu droplet during free fall is described by Curve *i* [8, 9]. As indicated by the right-hand ordinate of Figure 3, oxidation rates span a range of almost 10<sup>9</sup>.

Catalytic enhancement of plutonium corrosion by hydride significantly increases the risk associated with metal. The amount of oxide formed per day by exposing a kilogram-sized casting to air at 25°C varies from a few milligrams to a few micrograms depending on alloying and humidity. If hydride is present, the rate may be increased by a factor of  $10^7$  to  $10^{10}$ , resulting in complete reaction of a casting in 15 to 30 min. Reaction of N<sub>2</sub> during catalyzed corrosion eliminates boundary-layer control and R is four times that of self-sustained oxidation in static air. Hydride catalysis increases the rate of Pu+O<sub>2</sub> by as much as  $10^{13}$ , implying that catalyzed corrosion in air is throttled by slow reaction of nitrogen. In addition to an increase in the dispersal hazard, potential consequences of the catalyzed reaction include volume expansion of the solid and large thermal excursion.

As shown by particle-size data for different corrosion in Table 2 [15], the airborne release fraction is strongly dependent on reaction conditions. The mass fraction of small particles correlates strongly with reaction temperature, but the true correlation appears to be with reaction rate. Stress induced by formation of a low-density corrosion product on the metal surface is relieved by cracking and spallation of the product at a rate that seems largely independent of temperature. At low temperatures, corrosion is slow relative to spallation and a single distribution of small particles is formed. Relatively fast corrosion at high temperatures yields a distribution of large particles plus a distribution of small fragments formed during spallation. As expected, log-normal graphs of particle size vs. cumulative mass percent show single and bimodal distributions for the oxides formed at 25°C and 500°C, respectively. Appearance of a trimodal graph for Pu-PuH<sub>x</sub>+air at 500°C suggests that a third distribution of fine particles is formed by oxidation of nitride.

The particle size data in Table 2 show that large variations exist in airborne release fractions for oxides from metal. Though the bounding particle size for oxide entrainment remains unresolved, the mass fractions of dispersible particles vary by as much as  $10^6$  depending on product history. Reliable assessment of the dispersal hazard is unlikely if the origin of the oxide is not considered.

## **Conclusions**

Along with static and dynamic (explosive) oxidation of ignited plutonium, hydride-catalyzed corrosion of metal by air occurs within the time span of a credible incident and may substantially increase the dispersal hazard by metal. Unique features of catalyzed reaction are spontaneous initiation at low temperature and a large thermal excursion. Catalyzed reaction of oxygen is unusually rapid for a gas-solid process and merits further study to define transport processes, characterize products, and investigate potential application in the direct recovery of metal as oxide.

## References

1. C. A. Colmenares, Prog. Solid State Chem., **9** (1975) 139.
2. J. L. Stakebake, J. Less-Common Met., **123** (1986) 165.
3. J. L. Stakebake and L. A. Lewis, J. Less-Common Met., **136** (1988) 366.
4. J. L. Stakebake and M. A. Saba, J. Less-Common Met., **158** (1990) 221.
5. J. L. Stakebake, D. T. Larson, and J. M. Haschke, J. Alloys Comp. **202** (1993) 251.
6. J. M. Haschke, T. H. Allen, and J. L. Stakebake, J. Alloys Comp., **243** (1996) 23.
7. J. C. Martz, J. M. Haschke, and J. L. Stakebake, J. Nucl. Mater., **210** (1994) 130.
8. J. M. Haschke and J. C. Martz, "Oxidation of Plutonium in Air from 500 to 3500°C: Application to Source terms for Dispersal," Los Alamos Report LA-UR-97-360, Los Alamos National Laboratory, Los Alamos, NM, submitted for publication in Journal of Alloys and Compounds, 1997.
9. J. C. Martz and J. M. Haschke, "A Mechanism for Combustive Heating and Explosive Dispersal of Plutonium," Los Alamos Report LA-UR-97-361, Los Alamos National Laboratory, Los Alamos, NM, submitted for publication in Journal of Alloys and Compounds, 1997.
- 10 D. K. Knuth, DOE Safety Information Letter 93-05, U. S. Department of Energy, Washington, DC, December 1993.
11. J. M. Haschke and J. C. Martz, "Plutonium Storage," in Encyclopedia of Environmental Analysis and Remediation, John Wiley and Sons, New York, in press, 1997.
12. B. Hileman, Chem. Eng. News, **June 13** (1994) 23.
13. J. M. Haschke, "Hydrides," in Topics in f-Element Chemistry: Synthesis of Lanthanide and Actinide Compounds, Kluwer Academic Publishers, Dordrecht, Netherlands, 1991, Chapter 1.
14. F. Brown, H. M. Ockenden, and G. A. Welch, J. Chem. Soc., **1955** (1955) 4196.
15. T. E. Ricketts, Los Alamos National Laboratory, Los Alamos, NM, personal communication of unpublished data (1997).

Table 1. Arrhenius Equations<sup>a</sup> for Oxidation of Unalloyed and Alloyed Pu in Air and in Water Vapor.

| Curve | Reaction   | T Range (K) | A     | B      | Reference |
|-------|--|-------------|-------|--------|-----------|
| a     | Unalloyed Pu + H <sub>2</sub> O at P <sub>e</sub> <sup>b</sup> | 248-334     | 41.46 | 17,120 | 6         |
| b     | Unalloyed Pu + H <sub>2</sub> O <sup>c</sup>                   | 334-383     | 40.74 | 16,880 | 6         |
| d     | Unalloyed Pu + Dry Air <sup>d</sup>                            | < 673       | 13.68 | 9,010  | 6         |
| e     | Alloyed Pu + H <sub>2</sub> O <sup>c</sup>                     | 334-673     | 9.18  | 7,850  | 2, 3, 6   |
| f     | Alloyed Pu + Dry Air   | < 673       | 6.40  | 9,560  | 4, 6      |
| g     | Pu + Air <sup>d</sup> or H <sub>2</sub> O <sup>c</sup>         | 673-773     | 44.51 | 35,940 | 6         |
| h     | Static Pu + Air  | > 773       | -1.97 | 0      | 9         |
| i     | Dynamic Pu + Air   | 773-3773    | 4.21  | 4,830  | 9         |

a. Equations are for the linear stage of oxidation [6], and with the exception of Curve c for the transition region between 110 and 200°C have the form lnR (in g Pu/cm<sup>2</sup> min) = A - B/T.

b. P<sub>e</sub> is the equilibrium pressure of condensed water at T.

c. The H<sub>2</sub>O pressure is 160 Torr, the partial pressure of O<sub>2</sub> in air.

d. Dry air contains less than 0.5 ppm H<sub>2</sub>O.

Table 2. Size Distribution Data for Plutonium Oxide<sup>a</sup> Particles Formed by Corrosion of Pu Metal.

| Corrosion Reaction                                  | Cumulative Mass Fraction at Specified Size <sup>b</sup> |                    |                    |
|---|---|--------------------|--------------------|
|   | 3 $\mu\text{m}$   | 10 $\mu\text{m}$   | 30 $\mu\text{m}$   |
| Unalloyed Pu + Room Air at 25°C                     | 0.03  | 0.05               | > 0.95             |
| Pu + Air at 500°C                                   | 6x10 <sup>-6</sup>                                      | 5x10 <sup>-4</sup> | 1x10 <sup>-2</sup> |
| Pu-PuH <sub>x</sub> + Room Air at 25°C <sup>c</sup> | 6x10 <sup>-3</sup>                                      | 0.2                | 0.8                |
| Pu-PuH <sub>x</sub> + Air at 500°C                  | 5x10 <sup>-3</sup>                                      | 0.01               | 0.02               |
| Pu-PuH <sub>x</sub> + O <sub>2</sub> at 500°C       | 5x10 <sup>-5</sup>                                      | 2x10 <sup>-4</sup> | 2x10 <sup>-3</sup> |
| Pu Droplet Explosion at 3300°C                      | 0.7   | 0.8                | 0.8                |

a. Though residual PuH<sub>x</sub> and PuN may remain in products formed by hydride catalysis, particles with sizes less than 30  $\mu\text{m}$  probably oxidized to PuO<sub>2</sub> during handling in air.

b. Particle sizes are geometric; the aerodynamic equivalent diameter of a dioxide particle is about a factor of three larger than the geometric diameter.

c. Data are for a product formed without a large thermal excursion by slow reaction in a storage container.

## **Figure Captions**

Figure 1. Time dependence of pressure and gas temperature for reaction of air with plutonium hydride in a closed system.

Figure 2. Time dependence of pressure and gas temperature for reaction of air with an equimolar mixture of plutonium metal and hydride in a closed system.

Figure 3. Arrhenius curves for the reactions of unalloyed and alloyed (1 wt % Ga) plutonium with dry and moist air or water. Curves *a-g* are derived from References 6 and 9 and are identified in the text and in Table 1.

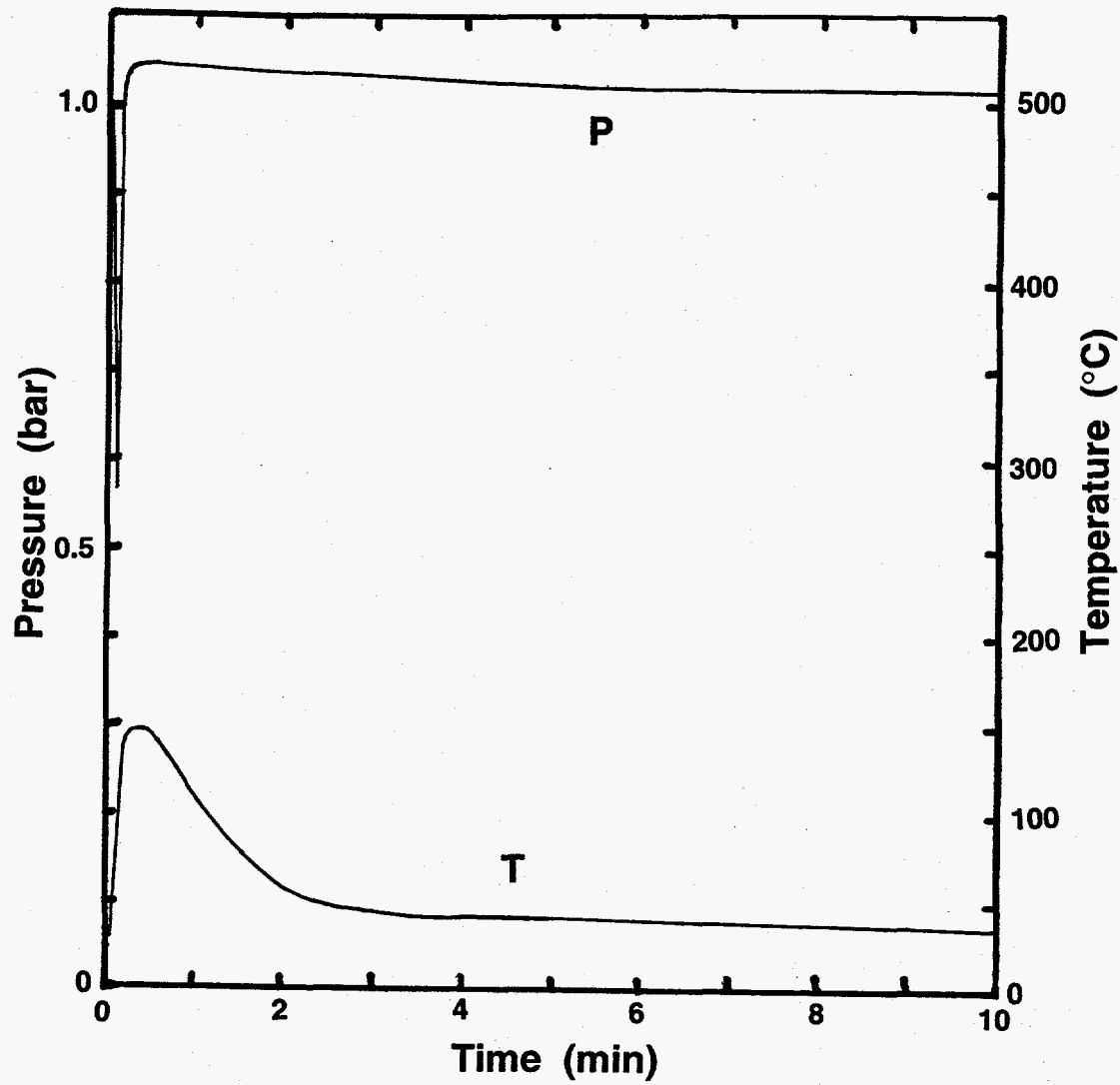


Figure 1. Time dependence of pressure and gas temperature for reaction of air with plutonium hydride in a closed system.

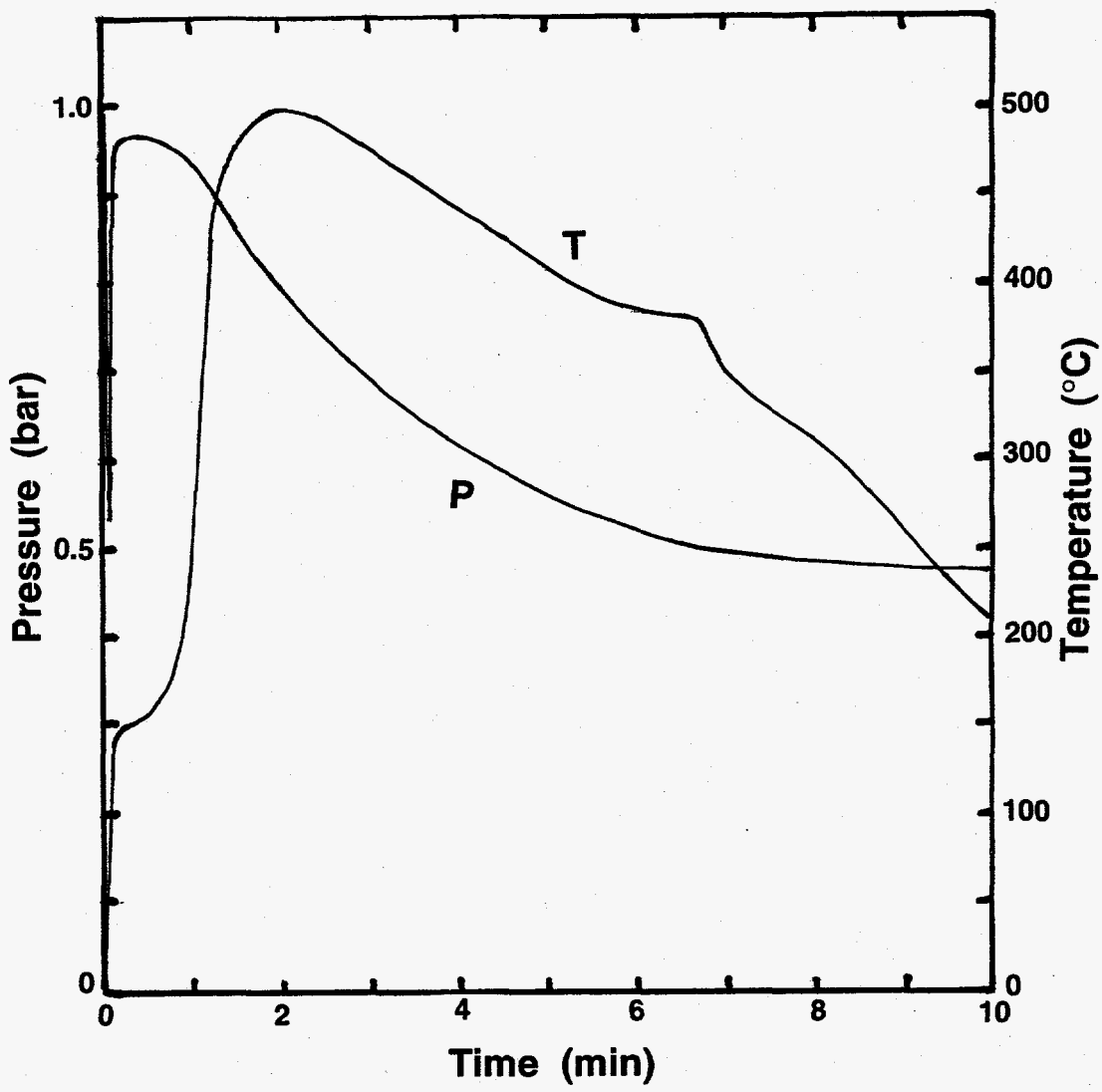


Figure 2. Time dependence of pressure and gas temperature for reaction of air with an equimolar mixture of plutonium metal and hydride in a closed system.

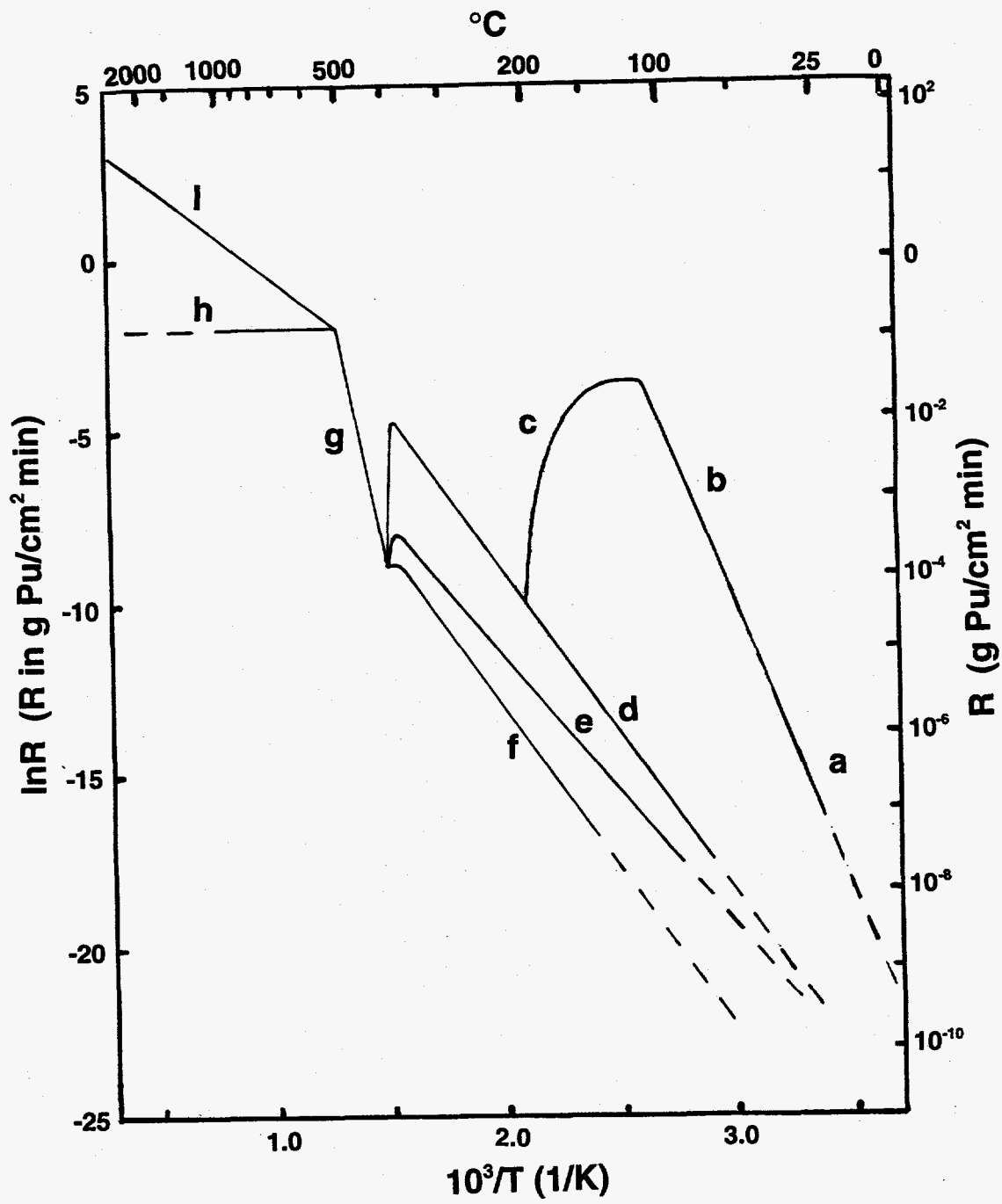


Figure 3. Arrhenius curves for the reactions of unalloyed and alloyed (1 wt % Ga) plutonium with dry and moist air or water. Curves *a-g* are derived from References 6 and 9 and are identified in the text and in Table 1.